Computational Mechanics (1991) 7, 329–339

Computational Mechanics

Two singular points finite elements in the analysis of kinked cracks

B. K. Dutta, A. Kakodkar
Reactor Engineering Division, Bhabha Atomic Research Centre, Bombay 400 085, India

S. K. Maiti
Department of Mechanical Engineering, Indian Institute of Technology, Bombay 400 076, India

Abstract. A formulation for incorporating two singular points (TSP) of variable orders in a single finite element is presented. Though the element does not satisfy any of the convergence criterion, its performance is found to be good, which has been demonstrated by considering number of examples on kinked cracks. In each case only one such element is incorporated in the whole discretization. These examples illustrate the usefulness of the element to analyse kinked cracks of various sizes and shapes and subjected to different loading and boundary conditions. Computed J-integrals are compared with analytical solutions, wherever possible, and the accuracy appears quite good. Effect of size of the element on, and the path independence of, J are also examined.

List of symbols

ξ, η	conventional natural coordinate system
ρ_1, ρ_2	another elemental natural coordinate system
L_{ij}	equation of side ij of an element
A_{ij}, B_{ij}	constants
N_i	shape function associated node i
λ_1, λ_2	constants associated with the order of singularities
α, β	an elemental natural coordinate system
u_i, v_i	displacement components in the Cartesian directions

1 Introduction

The finite element modelling of cracks of irregular shapes, e.g. zig–zag crack resulting from stress corrosion, is a difficult task. This is due to the fact that singularities exist at the corners, the order of which varies and depends on the knee angle (Williams 1952). The occurrence of the two adjacent singular points at close proximities further complicates the situation. One of the simplest problem in this family is a short kinked crack. The problem has received a considerable attention for analytical study, e.g., Badaliance (1981), Bilby and Cardew (1975), Chatterjee (1975), Cotterell and Rice (1980), Goldstein and Salganik (1976), Gupta (1975), Hussain et al. (1973), Khrapkov (1971), Lo (1978), Palaniswamy and Knauss (1978) and Vitek (1977). But it has not received much attention for finite element study. To analyse such a problem using the existing finite elements one obvious strategy is to use the wellknown quarter point square-root singularity elements (Barsoum 1976) at the crack-tip and a variable order singularity elements at the knee. Various approaches to develop a variable order singularity elements are very systematically reviewed by Atluri and Nakagaki (1986). An element, which is readily available and can be used at the knee, is due to Tracey and Cook (1977). This element meets the rigid body mode and the compatibility condition but not the constant strain requirement of the convergence criteria. In this strategy, from the point of view of accuracy, the two singularity elements must be separated by a set of conventional elements. When the kink length is small, the analyst is forced to use a very large number of elements and hence the computational cost increases. One alternative strategy is to employ a single element incorporating the two singularities between the knee and the crack-tip. This provided the motivation for the development of the two singular points finite element.

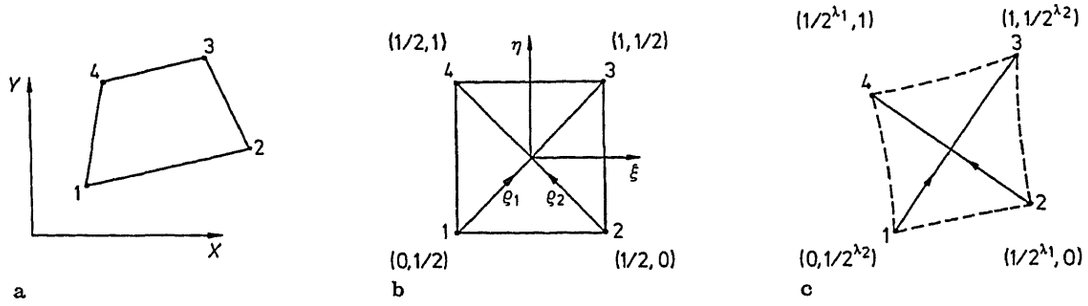

Fig. 1a–c. Illustration used to derive the displacement shape functions for a *TSP* element

We have had some success in developing such an element (Dutta et al. 1989a, b). We present here the formulation of the element and its performance in a number of cases.

2 Element formulation

Consider a 4-noded quadrilateral element as shown in Fig. 1a. The element can be mapped into a square in the conventional (ξ, η) system of natural coordinates (Fig. 1b). Consider now a local coordinate system (ρ_1, ρ_2) defined by

$$\rho_1 = (2+\xi+\eta)/4 \quad \text{and} \quad \rho_2 = (2-\xi+\eta)/4. \tag{1}$$

In this (ρ_1, ρ_2) system the coordinates of the four corner nodes are shown in Fig. 1b. The equations of four sides of the element are

$$\begin{aligned} L_{12} &= \rho_1+\rho_2-0.5=0, && \text{for side 1-2,}\\ L_{23} &= -\rho_1+\rho_2+0.5=0, && \text{for side 2-3,}\\ L_{34} &= \rho_1+\rho_2-1.5=0, && \text{for side 3-4,} \end{aligned} \tag{2}$$

and

$$L_{41} = -\rho_1+\rho_2-0.5=0, \quad \text{for side 4-1.}$$

The conventional shape functions associated with the four corner nodes can be written as

$$\begin{aligned} N_1 &= -(-\rho_1+\rho_2+0.5)(\rho_1+\rho_2-1.5) = C_1 L_{23} L_{34},\\ N_2 &= (\rho_1+\rho_2-1.5)(-\rho_1+\rho_2-0.5) = C_2 L_{34} L_{41},\\ N_3 &= -(-\rho_1+\rho_2-0.5)(\rho_1+\rho_2-0.5) = C_3 L_{41} L_{12}, \end{aligned} \tag{3}$$

and

$$N_4 = (\rho_1+\rho_2-0.5)(-\rho_1+\rho_2+0.5) = C_4 L_{12} L_{23}.$$

Note that $C_1 = C_3 = -1$ and $C_2 = C_4 = 1$. These are obtained from the fact that N_i is 1 at node $i, i = 1, 2, 3$ and 4. Consider a mapping $\alpha = \rho_1^{\lambda_1}$ and $\beta = \rho_2^{\lambda_2}$. α and β form an orthogonal system of coordinates. The element in the (α, β) system is shown in Fig. 1c. The equation of four straight lines joining the nodes are

$$\begin{aligned} L_{ij} &= A_{ij}\alpha + \beta + B_{ij}\\ &= A_{ij}\rho_1^{\lambda_1} + \rho_2^{\lambda_2} + B_{ij} \end{aligned} \tag{4}$$

where A_{ij} and B_{ij} are constants. Four shape functions can be then constructed using (3). C_i is adjusted such that N_i is unity at node i. These shape functions are given below explicitly.

$$\begin{aligned} N_1 &= C_1(A_{23}\rho_1^{\lambda_1} + \rho_2^{\lambda_2} + B_{23})(A_{34}\rho_1^{\lambda_1} + \rho_2^{\lambda_2} + B_{34}),\\ N_2 &= C_2(A_{34}\rho_1^{\lambda_1} + \rho_2^{\lambda_2} + B_{34})(A_{41}\rho_1^{\lambda_1} + \rho_2^{\lambda_2} + B_{41}),\\ N_3 &= C_3(A_{41}\rho_1^{\lambda_1} + \rho_2^{\lambda_2} + B_{41})(A_{12}\rho_1^{\lambda_1} + \rho_2^{\lambda_2} + B_{12}), \end{aligned}$$

and

$$N_4 = C_4(A_{12}\rho_1^{\lambda_1} + \rho_2^{\lambda_2} + B_{12})(A_{23}\rho_1^{\lambda_1} + \rho_2^{\lambda_2} + B_{23}) \tag{5}$$

where

$$A_{12} = 2^{\lambda_1}/2^{\lambda_2}$$
$$B_{12} = -1/2^{\lambda_2}$$
$$C_1 = [2^{2\lambda_2}(1-2^{\lambda_1})^2]/[2^{2\lambda_1}(1-2^{\lambda_2})]$$
$$A_{23} = 2^{\lambda_1}/[2^{\lambda_2}(1-2^{\lambda_1})]$$
$$B_{23} = 1/[2^{\lambda_2}(2^{\lambda_1}-1)]$$
$$C_2 = 1$$
$$A_{34} = [2^{\lambda_1}(1-2^{\lambda_2})]/[2^{\lambda_2}(1-2^{\lambda_1})]$$
$$B_{34} = [2^{\lambda_1}(2^{\lambda_2}-1)]/[2^{\lambda_2}(1-2^{\lambda_1})] - 1/2^{\lambda_2}$$
$$C_3 = 2^{2\lambda_2}/[2^{2\lambda_1}(1-2^{\lambda_2})]$$
$$A_{41} = 2^{\lambda_1}(1-2^{\lambda_2})/2^{\lambda_2}$$
$$B_{41} = -1/2^{\lambda_2}$$

and

$$C_4 = 1. \tag{6}$$

If the displacement field is written using these shape functions, i.e.

$$u = \sum_1^4 N_i u_i \quad \text{and} \quad v = \sum_1^4 N_i v_i$$

an incompatible element is obtained which displays strain/stress singularities at the corners 1 and 2. The orders of singularity are $-1+\lambda_1$ and $-1+\lambda_2$. These shape functions do not have any linear term when $\lambda_1 \neq 1$ and/or $\lambda_2 \neq 1$. Therefore the element cannot meet the constant strain condition of the convergence criteria. For a small distance between the two points 1 and 2, the contribution due to the singularities will dominate the exact solution and hence the exclusion of the linear term is inconsequential in the absence of thermal stresses.

The derivatives of the shape functions with respect to (ξ, η) are given by

$$\partial N_i/\partial\xi = \partial N_i/\partial\rho_1\,\partial\rho_1/\partial\xi + \partial N_i/\partial\rho_2\,\partial\rho_2/\partial\xi$$

and

$$\partial N_i/\partial\eta = \partial N_i/\partial\rho_1\,\partial\rho_1/\partial\eta + \partial N_i/\partial\rho_2\,\partial\rho_2/\partial\eta.$$

Using $\partial\rho_1/\partial\xi = 0.25$, $\partial\rho_2/\partial\xi = -0.25$, $\partial\rho_1/\partial\eta = 0.25$ and $\partial\rho_2/\partial\eta = 0.25$ these derivatives can be written finally in the following form.

$$\begin{aligned}
\partial N_1/\partial\xi &= C_1[\lambda_1\rho_1^{\lambda_1-1}[2A_{23}A_{34}\rho_1^{\lambda_1} + (A_{23}+A_{34})\rho_2^{\lambda_2} + (A_{23}B_{34}+A_{34}B_{23})] \\
&\quad - \lambda_2\rho_2^{\lambda_2}[(A_{34}+A_{23})\rho_1^{\lambda_1} + 2\rho_2^{\lambda_2} + (B_{34}+B_{23})]]/4. \\
\partial N_1/\partial\eta &= C_1[\lambda_1\rho_1^{\lambda_1-1}[2A_{23}A_{34}\rho_1^{\lambda_1} + (A_{23}+A_{34})\rho_2^{\lambda_2} + (A_{23}B_{34}+A_{34}B_{23})] \\
&\quad + \lambda_2\rho_2^{\lambda_2-1} + [(A_{34}+A_{23})\rho_1^{\lambda_1} + 2\rho_2^{\lambda_2} + (B_{34}+B_{23})]]/4 \\
\partial N_2/\partial\xi &= C_2[\lambda_1\rho_1^{\lambda_1-1}[2A_{34}A_{41}\rho_1^{\lambda_1} + (A_{34}+A_{41})\rho_2^{\lambda_2} + (A_{34}B_{41}+A_{41}B_{34})] \\
&\quad - \lambda_2\rho_2^{\lambda_2-1}[(A_{41}+A_{34})\rho_1^{\lambda_1} + 2\rho_2^{\lambda_2} + (B_{41}+B_{34})]]/4 \\
\partial N_2/\partial\eta &= C_2[\lambda_1\rho_1^{\lambda_1-1}[2A_{34}A_{41}\rho_1^{\lambda_1} + (A_{34}+A_{41})\rho_2^{\lambda_2} + (A_{34}B_{41}+A_{41}B_{34})] \\
&\quad + \lambda_2\rho_2^{\lambda_2-1}[(A_{41}+A_{34})\rho_1^{\lambda_1} + 2\rho_2^{\lambda_2} + (B_{41}+B_{34})]]/4 \\
\partial N_3/\partial\xi &= C_3[\lambda_1\rho_1^{\lambda_1-1}[2A_{41}A_{12}\rho_1^{\lambda_1} + (A_{41}+A_{12})\rho_2^{\lambda_2} + (A_{41}B_{12}+A_{12}B_{41})] \\
&\quad - \lambda_2\rho_2^{\lambda_2-1}[(A_{12}+A_{41})\rho_1^{\lambda_1} + 2\rho_2^{\lambda_2} + (B_{12}+B_{41})]]/4
\end{aligned}$$

$$\partial N_3/\partial\eta = C_3[\lambda_1\rho_1{}^{\lambda_1-1}[2A_{41}A_{12}\rho_1{}^{\lambda_1}+(A_{41}+A_{12})\rho_2{}^{\lambda_2}+(A_{41}B_{12}+A_{12}B_{41})]$$
$$+\lambda_2\rho_2{}^{\lambda_2-1}[(A_{12}+A_{41})\rho_1{}^{\lambda_1}+2\rho_2{}^{\lambda_2}+(B_{12}+B_{41})]]/4$$
$$\partial N_4/\partial\xi = C_4[\lambda_1\rho_1{}^{\lambda_1-1}[2A_{12}A_{23}\rho_1{}^{\lambda_1}+(A_{12}+A_{23})\rho_2{}^{\lambda_2}+(A_{12}B_{23}+A_{23}B_{12})]$$
$$-\lambda_2\rho_2{}^{\lambda_2-1}[(A_{23}+A_{12})\rho_1{}^{\lambda_1}+2\rho_2{}^{\lambda_2}+(B_{23}+B_{12})]]/4$$
$$\partial N_4/\partial\eta = C_4[\lambda_1\rho_1{}^{\lambda_1-1}[2A_{12}A_{23}\rho_1{}^{\lambda_1}+(A_{12}+A_{23})\rho_2{}^{\lambda_2}+(A_{12}B_{23}+A_{23}B_{12})]$$
$$+\lambda_2\rho_2{}^{\lambda_2-1}[(A_{23}+A_{12})\rho_1{}^{\lambda_1}+2\rho_2{}^{\lambda_2}+(B_{23}+B_{12})]]/4. \tag{7}$$

These derivatives show that there are singularities of orders $(-1+\lambda_1)$ and $(-1+\lambda_2)$ at the points $\rho_1\to 0$ and $\rho_2\to 0$ respectively.

For $\lambda_1=1$ and $\lambda_2=1, \sum_1^4 N_i=1$ and the element becomes an ordinary four noded quadrilateral and hence the rigid body mode and the constant strain condition are fully met. For $\lambda_1\neq 1$ and/or $\lambda_2\neq 1, \sum_1^4 N_i\neq 1$ and these two conditions are not satisfied. The failure to satisfy the constant strain condition renders the element unsuitable for thermal strain problems. This limitation is not all that serious under mechanical loadings because of the two singularities involved and reasons mentioned earlier. The failure to satisfy the rigid body mode may lead to straining of the element due to a rigid body motion of the nodes. To minimise the error, the element can perhaps be restrained from any significant rigid body motion. This can be done by tailoring the displacement boundary condition to fix one node of the TSP element. In all the case studies reported in Sect. 4 we have obtained results by adopting this method. In restraining the rigid body motion we have just restrained the rigid body translation.

We present below a modification of element displacement field, which helps to improve its performance.

3 Modification of element displacement field

For a rigid body motion $u_1=u_2=u_3=u_4=1$, the movement at the centre, $\rho_1=\rho_2=1/2$, is $\sum_1^4 N_i=C_v$, say. The error in the rigid body translation is $1-C_v$. We rewrite the element displacement field in the form

$$u=\sum_1^5 N_j u_j \quad v=\sum_1^5 N_j v_j \tag{8}$$

where $N_5=\rho_1{}^{\lambda_1}(1-\rho_1{}^{\lambda_1})\rho_2{}^{\lambda_2}(1-\rho_2{}^{\lambda_2})C_\lambda(1-C_v)$,
$C_\lambda=2^{2(\lambda_1+\lambda_2)}/(2^{\lambda_1}-1)(2^{\lambda_2}-1)$,

u_5 and v_5 are two arbitrary parameters and can be treated as nodeless variables.

The derivatives N_5 with respect to ξ and η are given by

$$\partial N_5/\partial\xi = C_\lambda(1-C_v)[\lambda_1\rho_1{}^{\lambda_1-1}(1-2\rho_1{}^{\lambda_1})\rho_2{}^{\lambda_2}(1-\rho_2{}^{\lambda_2})-\rho_1{}^{\lambda_1}(1-\rho_1{}^{\lambda_1})\lambda_2\rho_2{}^{\lambda_2-1}(1-2\rho_2{}^{\lambda_2})]/4,$$

and

$$\partial N_5/\partial\eta = C_\lambda(1-C_v)[\lambda_1\rho_1{}^{\lambda_1-1}(1-2\rho_1{}^{\lambda_1})\rho_2{}^{\lambda_2}(1-\rho_2{}^{\lambda_2})+\rho_1{}^{\lambda_1}(1-\rho_1{}^{\lambda_1})\lambda_2\rho_2{}^{\lambda_2-1}(1-2\rho_2{}^{\lambda_2})]/4. \tag{9}$$

Since u_5 and v_5 are nodeless variables and are associated with the element only, they can be condensed at the element level before the assembly of element stiffness matrices.

4 Examples

The element has been incorporated in a 2-D finite element code 'CRACK' (Dutta 1986) along with

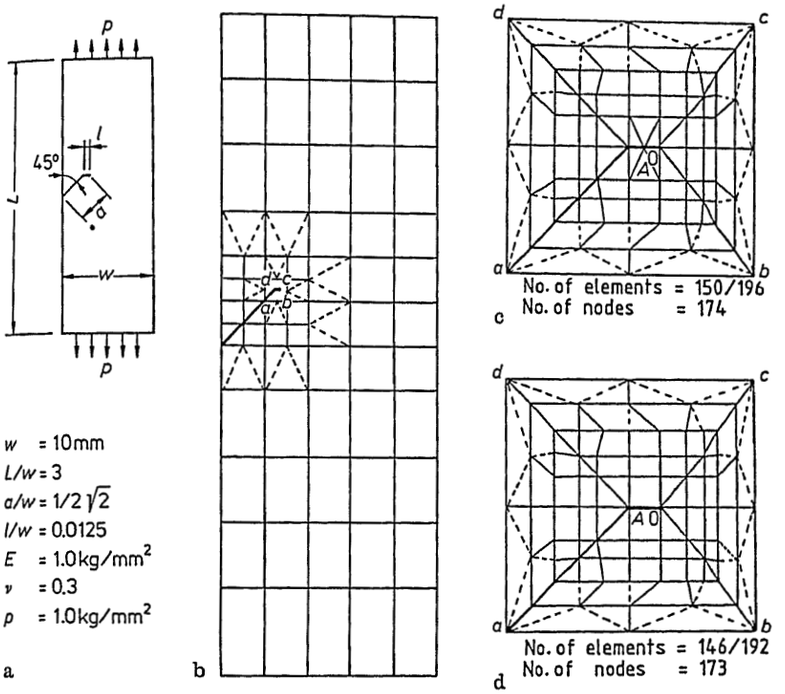

Fig. 2. a Single edge kinked crack in a long tension strip; b discretization details away from the knee and crack tip; c and d two discretization schemes around the knee and crack tip

the displacement modification. Results on few kinked cracks are presented below. Plane stress condition is assumed.

The first example deals with a kinked crack in a long elastic tension strip. The kink length $l = 0.035a$. The dimensional details are shown in Fig. 2. This problem has also been studied by Tracey and Cook (1977). The tip of the crack has the singularity with $\lambda_1 = 0.5$, while for the knee $\lambda_2 = 0.674$. Tracey and Cook (1977) have used the 3-noded triangular variable order singularity elements around the crack-tip and at the knee to model the two singularities. Apparently ten elements are used in between the knee and the crack-tip.

In the present study two discretization schemes around the knee and crack-tip (Fig. 2) were used. In the first case triangular elements are used in between the knee and crack-tip and in the second case only one rectangular element is used. Stress intensity factor was calculated with and without imposition of singularities at the tip of the kink and the knee. Stress intensity factors were calculated by comparing the displacement in the direction of loading at the first corner node A (Fig. 2) on the crack face and at the back of the crack-tip O. These results are shown in Table 1. The best result is obtained using the TSP element. The accuracy decreases if the proposed modification is not incorporated.

There is some incompatibility between regular elements in the discretization (Fig. 2). This was eliminated[1] by introducing more CST elements. The related extra nodal connections are shown by dotted lines. The results obtained after this modification are also presented in Table 1. In the last column (Table 1) a change of only 3.4% is observed.

The second example is of a kinked crack of the type shown in Fig. 3a. The order of singularity at the knee changes with the kink angle θ (Williams 1952). We examined θ in the range 15° to 90° in steps of 15°.

The discretization details are shown in Fig. 3 for the kink length $l = 0.04a$. The arrangements of elements around the crack tip and the knee for the cases $\theta = 90°$ and 45° are shown in Figs. 3c

[1] On the recommendation of one of the reviewers

Table 1. Computed values of mode-I SIF for single edge kinked crack in a long tension strip

Tracey and Cook (1977)	Computed SIF (kg·mm$^{-3/2}$) using discretization schemes				
	Triangular elements (Fig. 2c)		Rectangular elements (Fig. 2d)		
				Singularities imposed	
	Singularities not imposed	Singularities imposed	Singularities not imposed	TSP element without modification	TSP elements
2.317	1.720 (1.658)[a]	2.081 (2.000)	2.068 (1.997)	2.248 (2.167)	2.332 (2.254)

[a] Results within parentheses are obtained after eliminating the incompatibility between regular elements

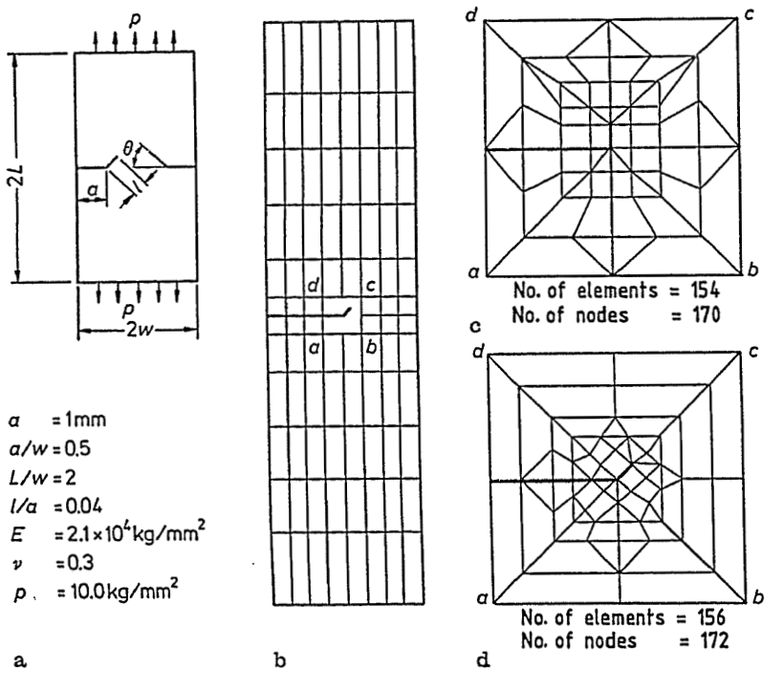

Fig. 3. a Double edge kinked cracks in a tension strip; b, c and d discretization details

and d respectively. The discretization scheme shown in Fig. 3d was used to study the cases $\theta = 75°$, 60°, 45°, 30° and 15°. For the cases $\theta = 75°$, 60°, 30° and 15° the coordinates of the nodes around the tip and the knee were suitably modified. Most of these elements are 4-noded quadrilaterals. Few CST elements are used in the transition zones between the coarse and finely discretized regions. The J-integral was computed using three different contours around the crack-tip (Fig. 4). These results are compared with those based on an analytical solution due to Cotterell and Rice (1980) in Table 2. The accuracy obtained is good.

The same problem was studied where the kink length $l = 0.02a$. The same discretization schemes (Fig. 3) with appropriate modification of relevant nodal coordinates have been used. The results are shown in Table 3. The values of J do not change appreciably in response to this reduction in length. This justifies the comparison with analytical results (Cotterell and Rice 1980), which are valid for very small kink length.

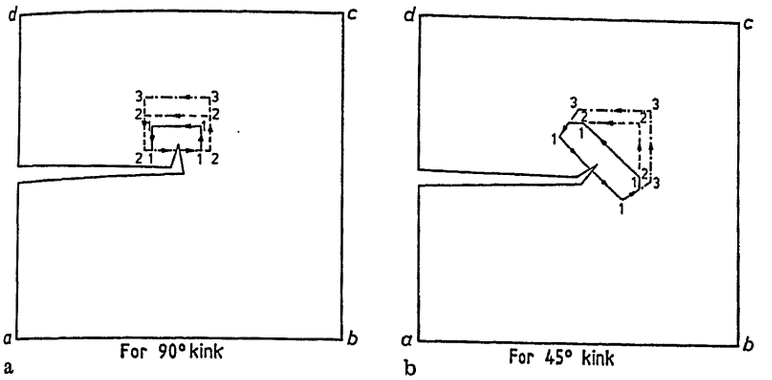

Fig. 4. J integral contorus for the double edge kinked crack problem

Table 2. Computed J-integral for 4% kink length for the double edge kinked crack problem

θ	λ at knee	Analytical (Cotterell and Rice 1980)	Computed J (kg-mm/mm^2) using TSP element		
			Based on different contours	Average	% differences with analytical solution
15°	0.85733	0.019858	0.01968 0.01901 0.02042	0.01963	−1.11
30°	0.751975	0.01789	0.01761 0.01751 0.01856	0.017893	+0.018
45°	0.673584	0.01497	0.01563 0.01522 0.01569	0.01544	+3.18
60°	0.615712	0.01156	0.01169 0.01171 0.01191	0.01177	+1.81
75°	0.573868	0.00814	0.007761 0.007945 0.0077414	0.0078158	−3.98
90°	0.544484	0.005138	0.004656 0.004836 0.005079	0.004857	−5.47

The third example is that of a 4-point bend specimen configuration (Fig. 5a). The study is done for θ in the range 15° to 90° in steps of 15°. The mesh arrangement is similar to the discretization schemes shown in Fig. 3. The J-integral was computed using three different contours around the crack tip. The average of computed J values are compared with the first order analytical solution (Cotterell and Rice 1980) in Fig. 5b.

The fourth example consists of a 3-point bend specimen configuration (Fig. 6a). The study was done in this case along the lines similar to that of 4-point bend specimen. The average of computed J values are compared with the analytical solution (Cotterell and Rice 1980) in Fig. 6b.

The last example (Fig. 7) deals with an asymmetrically branched crack in an infinite plate subjected to unidirectional tensile load. The case of 45° branched crack was only examined here. For the proportion shown in Fig. 7 the plate can very well be treated as an infinite body. The discretization scheme employed is shown in Fig. 7. In this analysis the kink dimension was held constant but the main crack length was varied. The first case was considered with the main crack extending from 1 to 9 and the kink extending from 9 to 10 (Fig. 7). For the second case left hand

Table 3. Computed J-integral for 2% kink length for the double edge kinked crack problem

θ	Analytical (Cotterell and Rice 1980)	Computed J (kg-mm/mm^2) using TSP element		
		Based on different contours	Average	% differences with analytical solution
15°	0.019858	0.01940 0.01894 0.02034	0.01956	−1.5
30°	0.01789	0.01777 0.01768 0.01873	0.01806	+0.95
45°	0.01497	0.01562 0.01548 0.01594	0.01568	+4.74
60°	0.01156	0.01181 0.01182 0.01203	0.1188	+2.8
75°	0.00814	0.0076117 0.0077968 0.0076035	0.0076706	−5.76
90°	0.005138	0.004233 0.004510 0.004687	0.0044766	−12.8

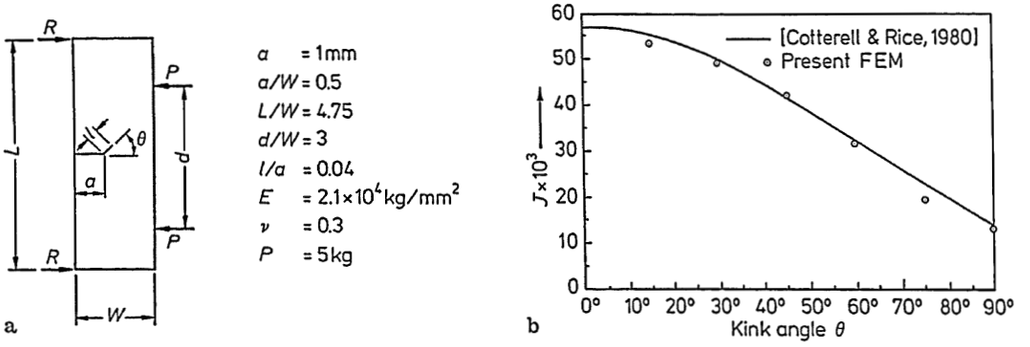

Fig. 5. **a** Single edge kinked crack under four point bending; **b** comparison of computed J with an analytical solution

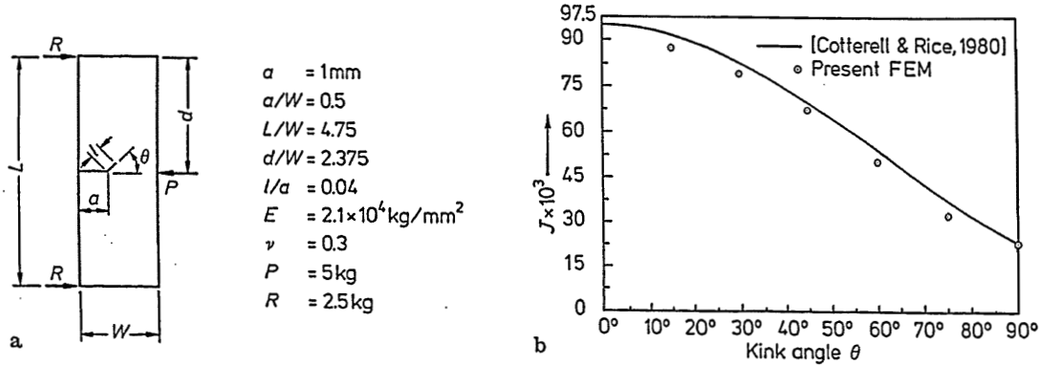

Fig. 6. **a** Single edge kinked crack under three point bending; **b** comparison of computed J with an analytical solution

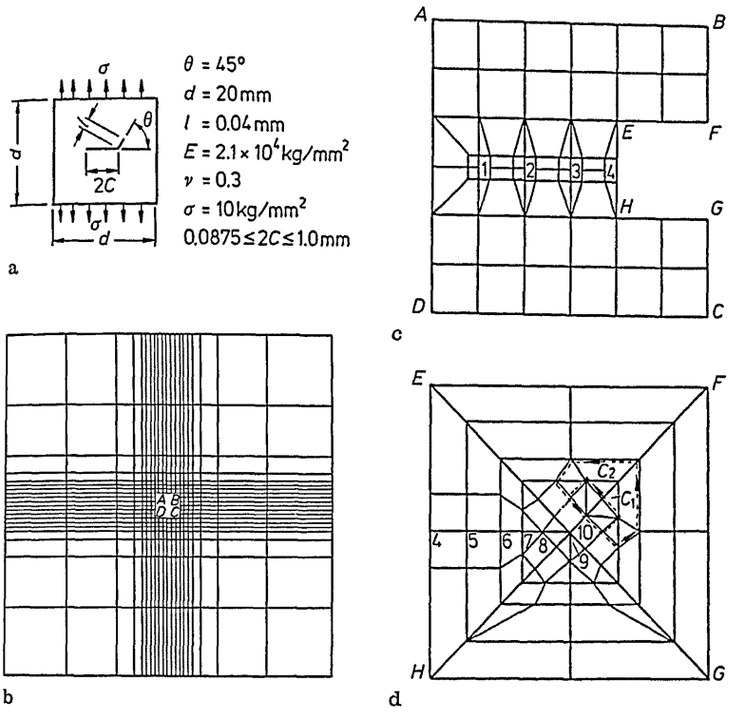

Fig. 7. a Asymmetrically branched crack in an infinite plate under tension; b, c and d discretization schemes near to and away from the crack

tip of the main crack was shifted from location 1 to 2 and the appropriate pair of nodes lying between 1 and 2 were made to coalesce. Thus seven cases were studied by varying the left hand tip locations from 1 to 7 (Fig. 7). J integral was computed along three different contours. A comparison with the results of Lo (1978) is presented in Table 4 and Fig. 8 for different c/l ratios. Lo's (1978) results, which are quoted in terms of K_I and K_{II} were converted in terms of J for this comparison.

5 Discussion and conclusions

The formulation given above presents a radical approach for modelling arbitrary singularities occurring at any two neighbouring points in a domain by a single element. The new element offers a very elegant and computationally advantageous way of modelling a propagating crack and zig–zag crack, that is handled in a step-by-step analysis, short kinked cracks, corrosion cracks, etc. The element formulation is straightforward and can be easily incorporated in a displacement based finite element package. The TSP element perform better than the element without the displacement field modification. We believe that the method of modification proposed can be used in other elements displaying rigid body error.

The element does not meet the rigid body mode. By a proper specification of the boundary displacement condition the rigid body motion of the element can be minimised and this, in turn, will help to contain the spurious energy mode. If the element is employed to analyse problems with a small kink length the error due to exclusion of the constant strain term becomes inconsequential because, under such a situation, the singular term dominates the exact solution.

It must be emphasized here that there is only one TSP element in the whole discretization. The size of the TSP element is fixed for a given kink length. Any mesh convergence study will mean refining the element surrounding the special element. Such a mesh convergence study was done and has been reported (Dutta et al. 1989). It is relevant to note here that refining the elements surrounding the TSP in the second example did not lead to any significant change in the computed

Table 4. Comparison of analytical and computed J for the case of asymmetrically branched crack in an infinite plate

C	C/l	Computed J (kg-mm/mm^2)		EJ average	EJ	% difference
		Based on different contours	average	$\sigma^2\pi C$	$\sigma^2\pi C$ Lo (1978)	
0.5	12.5	0.005123 0.005042 0.005232	0.0051323	0.68614	0.68112	+0.73
0.375	9.375	0.003874 0.003815 0.003951	0.0038	0.691623	0.68731	+0.62
0.25	6.25	0.002630 0.002594 0.002677	0.0026336	0.70419	0.69719.	+1.00
0.125	3.125	0.001416 0.001402. 0.001434	0.0014173	0.75793	0.74126	+2.25
0.09375	2.34375	0.001128 0.001119 0.00114	0.001129	0.80499	0.77339	+4.08
0.0625	1.5626	0.000837 0.0008332 0.0008446	0.00083826	0.89654	0.83969	+6.77
0.04375	1.09375	0.0006243 0.0006239 0.000631	0.0006264	0.95706	0.92603	+3.35

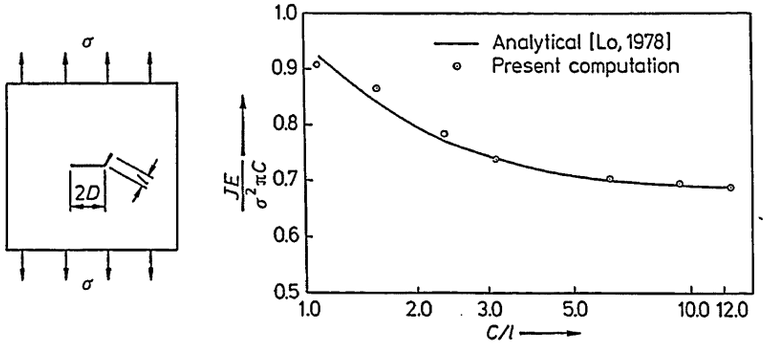

Fig. 8. Comparison of analytical and computed J for the case of asymmetrically branched crack in an infinite plate

J values. This means that while using the TSP element it is not necessary to use a very refined discretization to get a reasonably accurate solution.

Through the case studies, kinked cracks of various shapes and sizes subjected to different types of loading have been analysed. The computed results compare well with the numerical and/or analytical results. On the whole therefore, the TSP element has been found to be very useful in analysing the reported kinked crack problems.

References

Atluri, S. N.; Nakagaki, M. (1986): Computational methods for plane problems of fracture. In: Atluri, S. N. (ed): Computational methods in the mechanics of fracture, pp. 169–222. Amsterdam: North-Holland

Badaliance, R. (1981): Mixed mode fatigue crack propagation. In: Sih, G. C. (ed): Mixed mode crack propagation. Sijthoff and Noordhoff

Barsoum, R. S (1976): On the use of isoparametric finite elements in linear fracture mechanics. Int. J. Numer. Methods Eng. 10, 25–37
Bilby, B. A.; Cardew, C. E. (1975): The crack with a kinked tip. Int. J. Fract. 11, 708–712
Chatterjee, S. N. (1975): The stress field in the neighbourhood of branched crack in an infinite sheet. Int. J. Solids Struct. 11, 521–538
Cotterell, B.; Rice, J. R. (1980): Slightly curved or kinked cracks. Int. J. Fract. 16, 155–169
Dutta, B. K.; Kakodkar, A.; Maiti, S. K. (1986): Development of a computer code CRACK for elastic and elastoplastic fracture mechanics analysis of 2-D structure by finite element technique. BARC-1346
Dutta, B. K.; Maiti, S. K.; Kakodkar, A. K. (1989a): Development and application of two singular points finite elements. Int. J. Numer. Methods. Eng. 28, 1449–1460
Dutta, B. K.; Maiti, S. K.; Kakodkar, A. K. (1989b): Use of two singular points finite elements in the analysis of kinked cracks. Proc. 7th Int. Conf. Fracture, Houston, 3, 2315–2322
Goldstein, R. V.; Salganik, R. L. (1974): Brittle fracture of solids with arbitrary cracks. Int. J. Fract. 10, 507–523
Gupta, G. D. (1975): Strain energy release rate for mixed mode crack problems. ASME 75-WA/PVP-7
Hussain, M. A.; Pu, S. L.; Underwood, J. (1973): Strain energy release rate for a crack under combined mode I and II. ASTM STP 560, 2–28
Khrapkov, A. A. (1971): The first basic problem for a notch at the apex of an infinite wedge. Int. J. Fract. 7, 373–382
Lo, K. K. (1978): Analysis of branched cracks. J. Appl. Mech. 45, 797–802
Palaniswamy, K.; Knauss, W. G. (1978): On the problem of crack extension in brittle solids under general loading. In: Nemat-Nasser, S. (ed): Mechanics today, vol. 4, pp. 87–148. London: Academic Press
Tracey, D. M.; Cook, T. S. (1977): Analysis of power type singularities using finite elements. Int. J. Numer. Mech. Eng. 11, 1225–1233
Vitek, V. (1977): Plaine strain stress intensity factors for branched cracks. Int. J. Fract. 13, 481–501
Williams, M. L. (1952): Stress singularities resulting from various boundary conditions in angular corners of plates in extension. J. Appl. Mech. 19, 526–528

Communicated by S. N. Atluri, December 8, 1989